Mesomorphism, Polymerization, and Chirality Induction in α-Cyanostilbene-Functionalized Diacetylene-Assembled Films: Photo-Triggered *Z*/*E* Isomerization

Yan Zhang, Jingang Hu, Guang Yang, Hongli Zhang, Qijin Zhang, Feng Wang, Gang Zou

CAS Key Laboratory of Soft Matter Chemistry, Department of Polymer Science and Engineering, iChEM, University of Science and Technology of China, Hefei, Anhui 230026, People's Republic of China
Correspondence to: G. Zou (E-mail: gangzou@ustc.edu.cn) or F. Wang (E-mail: drfwang@ustc.edu.cn)

Received 8 February 2017; accepted 7 April 2017; published online 00 Month 2017
DOI: 10.1002/pola.28633

ABSTRACT: Engineering of molecular stacking arrangement via environmental stimuli is of particular interest in stimuli-responsive self-assembling architectures. A novel dual photo-functionalized diacetylene ((*Z*)-CNBE-DA) molecule was synthesized, in which photo-responsive cyanostilbene moieties exhibited interesting *Z*-*E* isomerization upon UV light irradiation and could be utilized to modulate mesomorphism, molecular stacking arrangement and their resulting polymerization behavior. Rod-like (*Z*)-CNBE-DA could self-assemble into well-defined lamellar structures and the helical polydiacetylene (PDA) chains could be formed upon irradiation with circularly polarized ultraviolet light (CPUL). However, the bent-shaped (*E*)-CNBE-DA molecules only self-assembled into irregular loose packing, inhibiting the formation of ordered helical PDA chains upon CPUL irradiation. In this work, we established the links between chemical structures, molecular packing engineering and photophysical properties, which would be of great fundamental value for the rational design of smart soft materials. © 2017 Wiley Periodicals, Inc. J. Polym. Sci., Part A: Polym. Chem. **2017**, *00*, 000–000

KEYWORDS: chiral; cyanostilbene; isomer/isomerization; liquid crystal; photoisomerization; photopolymerization; polydiacetylene

INTRODUCTION Over the past few decades, stimuli-responsive chiral self-assembling architectures continue to be a hot topic, since chirality is a basic character of nature and the chiral assemblies have emerged as the primary building blocks for the design of chiral functional materials at various hierarchical levels.[1–4] Of particular interest is engineering of molecular stacking arrangement via environmental stimuli rather than the variation of their primary chemical structure. Therefore, fine-tuning the intermolecular interaction and subsequently controlling of the molecular stacking arrangement, have been regarded as a promising approach to control the optoelectronic properties of the functional conjugated organic materials.[5–7] Polydiacetylene (PDA) is one of the most interesting conjugated organic materials due to its unique environmentally responsive optical characteristics and the promising application in optics,[8] electronics,[9,10] chemosensors,[11,12] and biosensors.[13–15] As is well known, the topo-chemical polymerization of the diacetylene (DA) monomer is very sensitive to the molecular stacking arrangement and orientation (the monomer diyne units should be arranged with a repeat distance of 5 Å and an orientation angle of 45 °C relative to the translation axis).[16] So far, various types of functional groups have been incorporated into diacetylene monomer, and a variety of experimental and theoretical works have been carried out to manipulate the well-defined molecular architectures.[17–19] However, there were few reports concerning on the links among the mesomorphism, polymerization and chirality induction in DA assemblies.[20] In particular, control of the mesomorphic and crystalline organization in diacetylene assemblies via photo-triggered isomerization of photo-responsive α-cyanostilbene central core structure, and their resulting polymerization and chiral induction behavior have not been described to date.

Linear π-conjugated organic molecules consisting of α-cyanostilbene unit have been rapidly developed as an interesting molecules toward innovative optoelectronics devices applications, due to their peculiar photophysical and self-assembling characteristics.[21–24] The fluorescent behavior, known as aggregation-induced emission,[25,26] as well as their structural modulation upon reversible *trans–cis* photoisomerization have attracted enormous attention.[27–33] Extensive studies in this field are mainly focused on the (*Z*)-1-

Additional Supporting Information may be found in the online version of this article.

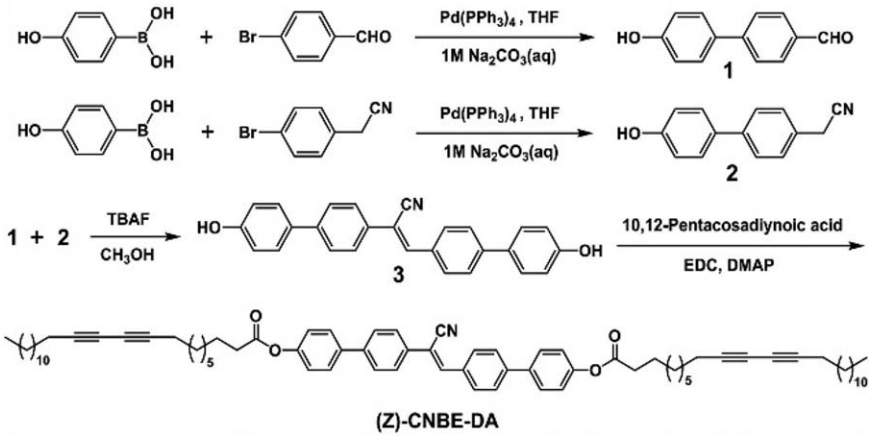

SCHEME 1 Synthetic routes of (Z)-CNBE-DA.

cyano-1,2-diphenyl-ethylene ((*Z*)-CNBE) derivatives, since they have strong π–π interactions between rigid rod-like aromatic segments and dipole interactions from polar cyano functionality group substituted on the vinyl group, controlling the molecular stacking to generate various supramolecular, mesomorphic, and crystalline organizations.[5,34–36] However, very little is known for the characteristics of (*E*)-CNBE derivatives, especially the modulation of their molecular self-assembled structure and mesomorphism via photo-triggered *Z-E* isomerization. Soo et al. reported the structural, photophysical, and thermal properties of the *trans* and *cis* isomers of (*Z*)-CN-MBE, which exhibited a reversible photo/thermal *Z-E* isomerization process, accompanied by a remarkable fluorescence on/off switching in the solid state.[28] Zhao et al. achieved *in situ* tuning luminescent color conversion along yellow, white, and blue based on cyanostilbene functionalized quantum dots by *Z-E* photo-isomerization.[33] In this article, it is anticipated that the introduction of α-cyanostilbene unit into DA system would fruit dual photo-functionalized materials (abbreviated as (*Z*)-CNBE-DA) with novel photo/thermal responsive properties, the mesomorphism, the molecular stacking arrangement, and the resulting polymerization behavior in the diacetylene assemblies could be easily controlled and modulated via photo-triggered *Z-E* isomerization of the CNBE core. Further, we achieved the chiral transference from the helical PDA backbone to the chiral arrangement of the CNBE core upon irradiation with circularly polarized ultraviolet light (CPUL). On the other hand, the desired chain configuration could be permanently locked by the polymerization of diacetylene groups to gain a deep insight into the structure–property relationship. Herein, it is realized that the construction of strong links between molecular packing arrangement and photochemical properties of the resulting molecules would be the core research for the development of smart and multifunctional soft materials.

EXPERIMENTAL

Materials

10,12-Pentacosadiynoic acid (DA) purchased from Tokyo Chemical Industry was purified by dissolving in dichloromethane and filtrating to remove the polymer before use. 4-hydroxyphenylboronic acid, 4-bromophenylace-tonitrile, 4-bromobenzaldehyde, Pd(PPh3)$_4$, 4-dimethylaminopyridine (DMAP), and 1-(3-dimethylaminopropyl)-3-ethylcarbodiimide hydrochloride (EDC) were purchased from Aldrich and used as received. Dichloromethane (DCM) was dried over anhydrous magnesium sulfate and filtered before use. All other solvents and reagents were of analytical grade and used as received. Milli-Q water (18.2 MΩ cm) was used in all cases.

Sample Preparation

4′-Hydroxy-biphenyl-4-carbaldehyde (1), (4′-hydroxy-biphenyl-4-yl)-acetonitrile (2), and (*Z*)-2,3-bis(4′-hydroxy-biphenyl-4-yl)-acrylonitrile (3) were synthesized according to the methods described in the ref. 37.

Compound 3: ^{1}H NMR (300 MHz, DMSO-d_6, δ, ppm): 8.02 (s, 1H), 7.98 (d, 2H, $J = 8.4$ Hz), 7.82–7.66 (m, 6H), 7.53 (t, 4H, $J = 9.0$ Hz), 6.76 (t, 4H, $J = 9.2$ Hz). FTIR (KBr, cm^{-1}): 3388 (OH), 3024 (C—CH), 2217 (CN).

(*Z*)-2,3-Bis(4′-(10,12-pentacosadiynoate)-biphenyl-4-yl)-acrylonitrile (abbreviated as (*Z*)-CNBE-DA) was synthesized in analogy to the following procedure and the molecular structure was shown in Scheme 1. DA (100 mg, 0.27 mmol), compound 3 (47 mg, 0.12 mmol), EDC (93mg, 0.48 mmol), and DMAP (13 mg, 0.11 mmol) were dissolved in 15 mL dry DCM. The reaction mixture was stirred at room temperature (RT) for 24 h under the protection of nitrogen. After removing the solvent, the residue was successively extracted with saline/DCM for three times, and the collected organic phase was dried with anhydrous magnesium sulfate. After solvent evaporation, the crude product was purified by column chromatography (silica gel, petroleum ether:DCM, 1:3) to obtain a white solid.

Yield: 70.5 mg, 48%. mp. 109 °C. ^{1}H NMR (300 MHz, $CDCl_3$, δ, ppm): 8.01 (d, 2H, $J = 8.3$ Hz), 7.79 (d, 2H, $J = 8.3$ Hz), 7.72 (s, 1H), 7.71–7.59 (m, 8H), 7.20 (dd, 4H, $J = 8.5$, 2.0 Hz), 2.60 (t, 4H, $J = 7.5$ Hz), 2.26 (q, 8H, $J = 6.5$ Hz), 1.87–1.71 (m, 4H), 1.26 (m, 60H), 0.95–0.83 (m, 6H). ^{13}C NMR (300 MHz, $CDCl_3$, δ, ppm): 172.24, 150.74, 141.27, 137.57, 133.46, 132.72, 129.89, 128.06, 126.42, 122.12, 118.04, 110.95, 65.35, 34.40, 31.92, 29.63, 24.91, 22.69, 19.21,

14.13. FTIR (KBr, cm^{-1}): 3061 (C═CH); 2921, 2850 (CH_2); 2223 (CN); 2175, 2139 (C≡C); 1747 (C═O); 1600, 1497, 1467. MALDI-MS (m/z): Calcd for $C_{27}H_{18}NO_2$, 388.13; Found, 388.97. Calcd for $C_{16}H_{26}$, 218.20; Found, 217.99.

Compound (*Z*)-CNBE-DA was dissolved in cyclopentanone with a concentration of 5 mg mL^{-1}. Then, the monomer films were prepared by the solution casting method. A few drops of the solution were added to the solid substrates. After solvent evaporation, the transparent monomer films were dried under vacuum (5 mmHg) at 50 °C for 12 h. All the preparation procedures descried above were performed in darkness to avoid polymerization in advance. A 365-nm UV light irradiation was employed to realize the *Z*–*E* photoisomerization of α-cyanostilbene mesogen within CNBE-DA monomer in the solution. A hand-held UV lamp (λ=254 nm) and circularly polarized UV light (CPUL, λ=313 nm) were used for normal UV polymerization or to prepare chiral polydiacetylene films, respectively. The crystalline colorless thin films of (*Z*)-CNBE-DA and the pale yellow thin films of (*E*)-CNBE-DA were both converted into blue PDA films. The films thickness were about 200 nm for (*Z*)-CNBE-DA and 225 nm for (*E*)-CNBE-DA by AFM (Supporting Information Fig. S5).

Characterization

^{1}H NMR and ^{13}C NMR spectra experiments were carried out with a JEOL FX-90Q NMR 300 spectrometer. FTIR experiments were performed on a MAGNA 750 FTIR spectrometer. Matrix-assisted laser desorption/ionization time-of-flight mass spectrum (MALDI-TOF-MS) was recorded on a Bruker BIFLEXe III mass spectrometer using a nitrogen laser (337 nm). The UV−vis absorption spectra were recorded on a SHIMADZU UV-2550 PC spectrophotometer. A Hamamatsu LC6 Hg/Xe lamp combined with a 313-nm interface filter and a 365-nm filter were used as the CPUL irradiation source and the UV irradiation source, respectively. Polarized optical microscopy (POM) images were obtained in an Olympus BX-51 fluorescence microscope equipped a heating stage with an INSTEC mK1000 high precision temperature controller. Differential scanning calorimetry (DSC) measurements were performed on a TA Instruments Q2000 DSC at a heating and cooling rate of 10 °C min^{-1} under nitrogen atmosphere. X-Ray diffraction (XRD) measurements were performed with a Rigaku AX-G by using a CuKα (λ=0.154 nm) beam. The Raman spectra were performed on a LABRAM-HR Confocal Laser MicroRaman Spectrometer with 514.5 nm radiation. The circular dichroism (CD) spectra were measured by using JASCO CD spectrometer J-810. Transmission electron microscopy (TEM) images were obtained in a JEOL-2000 microscope (operated at 200 kV). Atomic force microscope (AFM) images were recorded on Veeco diInnova microscope with a DAC controller.

RESULTS AND DISCUSSION

Morphology and Structural Characterization of CNBE-DA Films

The molecular structure and the synthetic routes of (*Z*)-CNBE-DA were presented in Scheme 1, detailed experimental details were shown in the Experimental section. The terminal diacetylene fragments were directly attached to the CNBE central core by esterification reactions to facilitate a mesomorphic organization.[5] The molecular structure of (*Z*)-CNBE-DA was confirmed by ^{1}H NMR, ^{13}C NMR, FTIR, and mass spectroscopy (Supporting Information Figs. S1–S4).

The optical characteristics of (*Z*)-CNBE-DA in solution were investigated by UV–vis absorption spectroscopy. The reversible photoisomerization of CNBE-DA was shown in Figure 1(a) upon irradiation with 365- and 254-nm UV light, respectively. The (*Z*)-CNBE-DA in THF solution exhibited the absorption maximum peak (λ_{max}) at 355 nm [black bold line in Fig. 1(c)], which was attributed to π–π* transition absorption of the chromophore CNBE core. Upon irradiation with 365-nm UV light (1.5 mW·cm^{-2}), the absorption maximum peak (λ_{max}) was gradually shifted from 355 to 340 nm, accompanied by a decrease of absorption intensity, and the photo-stationary state (PSS) was quickly achieved after approximately 15 s of 365-nm UV irradiation [Fig. 1(c)]. This blue-shift in the absorption should be ascribed to the *Z*→*E* isomerization, due to the reduction of effective conjugation length in the bent *E*-isomer conformation. Then upon irradiation with 254-nm UV light (0.07 mW·cm^{-2}), the opposite red-shift for the absorption λ_{max} and the partial recovery of the absorption intensity should be ascribed to the *E*→*Z* isomerization, and its absorbance increased until another equilibrium was reached after 50-s irradiation time [Fig. 1(d)]. We must note here that two absorbing species (*Z*- and *E*-isomer) were both present in this case since there was the isosbestic point appearing in the same position of 323 nm.[28] In addition, the *Z*→*E* and *E*→*Z* photoisomerization process could also be monitored by ^{1}H NMR characterization. At initial stage, CNBE-DA molecules were all in the *Z*-form [Fig. 1(b) (i)]. After irradiation with 365-nm UV light for 20 s, partial *Z*-form CNBE-DA molecules were transferred to the *E*-isomer, and the *Z*/*E* ratio could be estimated to be approximately 33/67 according to the ^{1}H NMR integral studies [Fig. 1(b) (ii)]. Then irradiation with 254-nm UV light for 60 s, only partial *E*-isomer could be transformed back to the *Z*-isomer, and the *Z*/*E* ratio was estimated to be about 55/45 [Fig. 1(b) (iii)]. Similar results could be obtained when monitored *Z*/*E* ratio by proton peak split of alkyl area connected with ester group (located in 2.6 ppm) according as the ^{1}H NMR integral studies.

The mesomorphism behavior of (*Z*)-CNBE-DA were studied by differential scanning calorimetry (DSC), polarized optical microscopy (POM) and X-ray diffraction (XRD) characterization, which revealed the presence of crystalline, nematic, and isotropic phases. As shown in Figure 2(a), (Z)-CNBE-DA molecules melted to the liquid crystal (LC) phase at about 109 °C (with a typical schlieren texture of nematic phase observed by POM, inset in Fig. 2(a)] and switched to isotropic phase at about 183 °C with a heating rate of 10 °C/min. During the cooling process with the same rate of 10 °C/min, two exothermic peaks were observed at approximately 178 and 91 °C with a wide LC phase temperature range,

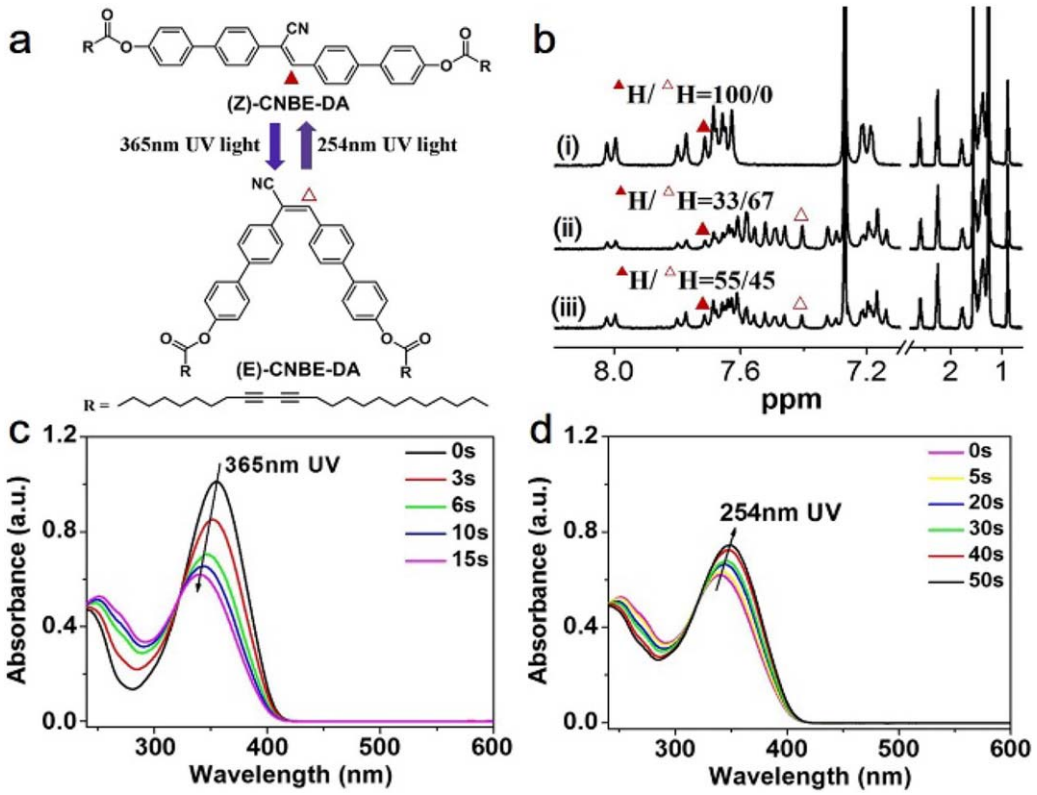

FIGURE 1 (a) Reversible photo-isomerization of CNBE-DA upon irradiation with 365- and 254-nm UV light, respectively. (b) ^{1}H NMR spectra changes of (*Z*)-CNBE-DA in $CDCl_3$: (i) before irradiation, (ii) upon 365-nm UV irradiation for 20 s and (iii) then 254-nm UV irradiation for 60 s. (protons in the vinylene of *Z*-isomer form (▲) and *E*-isomer form (△). UV–vis absorption spectra changes of (*Z*)-CNBE-DA in THF solution (2×10^{-5} M) upon irradiation with (c) 365-nm UV light (1.5 mW·cm^{-2}) and (d) then 254-nm UV light (0.07 mW·cm^{-2}). [Color figure can be viewed at wileyonlinelibrary.com]

ascribable to the isotropic to nematic phase transition, and the crystallization transition [with spherulites formation, inset in Fig. 2(a)], respectively. The XRD profile of (*Z*)-CNBE-DA in nematic phase at 120 °C was demonstrated in Figure 2(b), with a sharp and intense reflection at 1.75°, corresponding to layer spacing of 5.05 nm. The broad hump in the wide-angle region suggested the absence of in-plane positional order in LC phase.[38] Transmission electron microscopy (TEM) images for the (*Z*)-CNBE-DA assemblies in crystal state showed highly ordered lamellar structure (Supporting Information Fig. S6a). The incorporating of CNBE chromophore would reinforce the intermolecular interactions, resulting in the formation of regular lamellar aggregates structure. The formation of highly ordered crystal structure with an intense (001) reflection at 6.0 nm was demonstrated by small-angle XRD analysis [Fig. 2(c)], and layer spacing (d) with ratios of 1, 1/3, 1/4, and 1/6 characteristic for a lamellar phase, which were indexed as diffractions from the (001), (003), (004), and (006) planes, respectively.[39] In the wide angle region, a π–π stacking peak at the value of 19.2° could be observed, corresponding to a mean lateral spacing of 0.46 nm between the molecules [inset in Fig. 2(c)]. The extended molecular length (*L*) for (*Z*)-CNBE-DA was evaluated using Materials Studio calculation to be 7.5 nm, longer than d-spacing of 6.0 nm, suggesting the molecular arrangement in the layer must be tilted by an angle of 37° relative to the layer normal.[40] A schematic diagram of molecular packing arrangement of (*Z*)-CNBE-DA assemblies in crystal state was presented in Figure 2(d).

As we know, CNBE-based core could undergo *Z*→*E* isomerization upon 365-nm UV light irradiation. Therefore, it is anticipated that the *Z*→*E* isomerization of the CNBE-based core may influence the molecular packing arrangement as well as their mesomorphic behavior. The (*Z*)-CNBE-DA solution were irradiated with 365-nm UV light for 20 min and partial (*Z*)-CNBE-DA transformed into (*E*)-CNBE-DA. As indicated by DSC and POM characterization (Fig. 3a), this sample (pretreated with 365-nm light irradiation) melted to isotropic phase at about 108 °C with a heating rate of 10 °C/min. Continued slowly cooling with a same rate of 10 °C/min, the crystallization transition occurred at 92 °C with spherulites formation. No LC phase texture could be observed during the heating or cooling process. And that, highly ordered lamellar structures were broken for the sample treated with 365-nm UV light irradiation (Supporting Information Fig. S6b). During the assembly process, partial CNBE based core tended to adopt bent-shape structure, and the steric hindrance inhibited the formation of highly ordered molecular close-packing. Thus, no distinct morphology could be

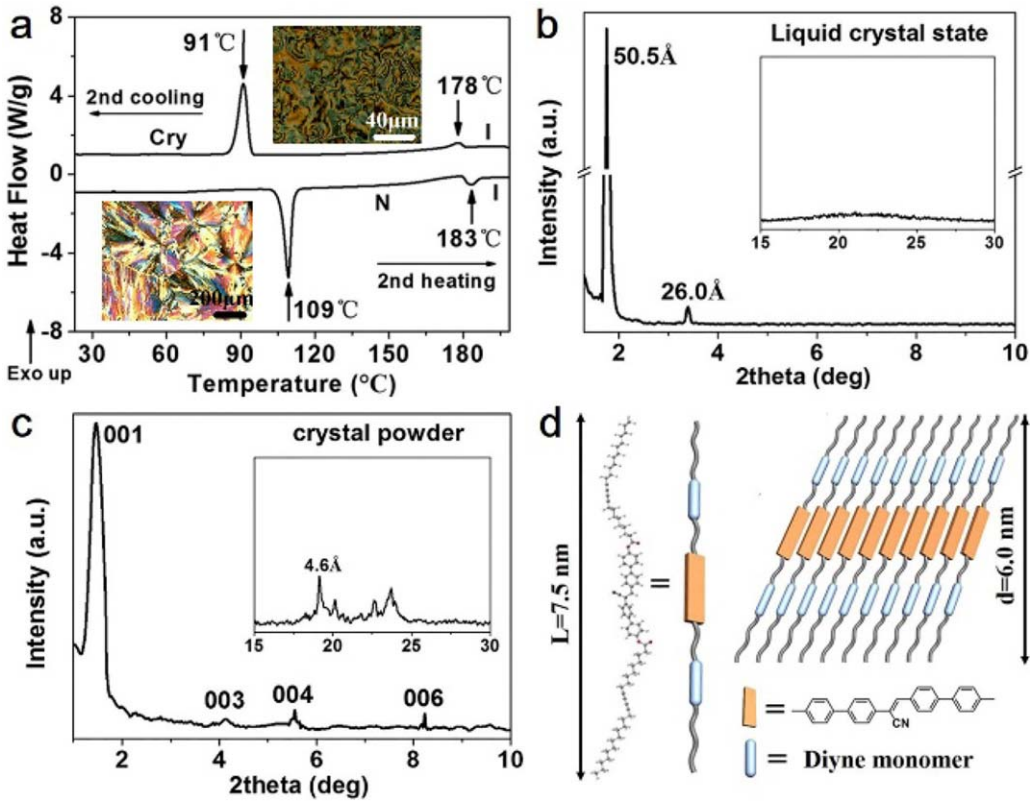

FIGURE 2 (a) DSC curve of (*Z*)-CNBE-DA on heating/cooling rate of 10 °C/min. The insets showed POM images of nematic phase and crystalline phase of (*Z*)-CNBE-DA during cooling (scale bar: 40 and 200 μm, respectively). (b) XRD pattern of (*Z*)-CNBE-DA in LC phase at 120 °C during cooling. (c) XRD pattern of (*Z*)-CNBE-DA crystal powder at 30 °C. (d) The packing model of a highly ordered lamellar structure of (*Z*)-CNBE-DA assemblies in crystal state. [Color figure can be viewed at wileyonlinelibrary.com]

observed in this case. XRD profile of the sample in the crystal state was shown in Figure 3(b), with a sharp and intense reflection at 1.52° and 1.77°, corresponding to layer spacing of 6.0 and 5.0 nm, indicating both of *Z*- and *E*- isomer were present in the crystal state. The energy-optimized structure of (*E*)-CNBE-DA was shown in Supporting Information Figure S7 by Materials Studio calculation, and the molecular length was calculated to be 5.1 nm close to the d-spacing of 5.0 nm. The simplified schematic illustration of photo-induced molecular conformation transformation was demonstrated in Figure 3(c). The proposed packing arrangement of a disordered structure of (*E*)-CNBE-DA assemblies deduced from XRD study was presented in Figure 3(d). Moreover, the photo-triggered phase transition for the (*Z*)-CNBE-DA sample from nematic phase to isotropic phase occurred within 5 min at 120 °C upon 365-nm UV irradiation (Supporting Information Fig. S8), which should be ascribed to the *Z*-*E* photo-isomerization of CNBE-based core. All above results indicated the molecular packing arrangement as well as the mesomorphic behavior of CNBE-DA assemblies could be easily controlled and modulated by 365-nm UV irradiation via *Z*-*E* photo-isomerization of CNBE-based core.

Enantio-Selective Polymerization of CNBE-DA Films

The diacetylene monomer could be polymerized under UV irradiation as detected optically by UV–vis absorption spectra characterization. (*Z*)-CNBE-DA films were prepared by the solution casting method. As expected, (*Z*)-CNBE-DA films could be polymerized upon irradiation with 254-nm UV light. Typically intense absorption maximum at about 645 and 590 nm, corresponding to the electronic transition of the conjugated π orbital of polydiacetylene (PDA) chain, improved with the increasing of the irradiation time [Fig. 4(a)], tending to be saturated after UV irradiation for 4 min. After polymerization, the fractional conversion value for the sample was about 0.37. The films exhibited two characteristic Raman vibrational bands at 2098 and 1496 cm^{-1}, corresponding to the C≡C and C═C stretching vibrations of PDA chain (Supporting Information Fig. S9). Time-depended development of absorption maximum at 645 nm was used to determine the polymerization kinetics of (*Z*)-CNBE-DA, which described as a first-order reaction with the polymerization rate constant k was 1.8×10^{-2} s^{-1} [Fig. 4(b)]. We found that (*Z*)-CNBE-DA could not be polymerized in nematic LC state since the (Z)-CNBE-DA monomers had a mobility and they could not be arranged in-plane positional order in LC phase, which disturbed the well-ordered stacking arrangement and orientation of diacetylene groups (Supporting Information Fig. S10). For the sample pretreated with 365-nm light irradiation, partial (*Z*)-CNBE-DA molecules were transformed into the *E*-isomer, and the steric hindrance would inhibit the highly ordered molecular packing, resulting

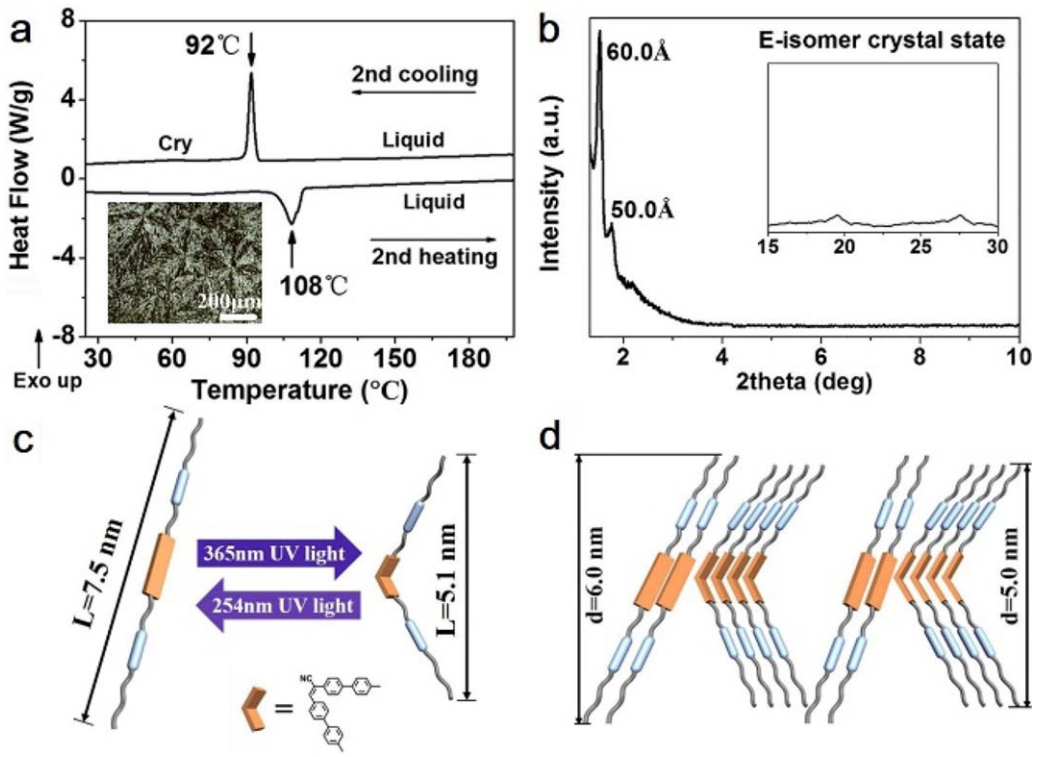

FIGURE 3 (a) DSC curve of (*E*)-CNBE-DA on heating/cooling rate of 10 °C/min. The inset showed POM image of crystalline phase of (*E*)-CNBE-DA during cooling (scale bar: 200 μm). (b) XRD pattern of (*E*)-CNBE-DA in crystal state at 30 °C. (c) Schematic illustration of photo-induced molecular conformation transformation. (d) The packing model of a disordered structure of (*E*)-CNBE-DA assemblies in crystal state. [Color figure can be viewed at wileyonlinelibrary.com]

in lower monomer conversion degree (0.13) and lower absorption intensity [Fig. 4(c)]. A slight blue-shift of the absorption maximum at 640 and 580 nm for PDA chain could be observed, due to the reduction of effective conjugation length for PDA chain. The polymerization rate constant k was calculated to be about 2.0×10^{-2} s^{-1} [Fig. 4(d)].

Moreover, we demonstrated that left- and right-handed circularly polarized UV light (CPUL) could be utilized to induce the enantioselective photo-polymerization of DA assemblies, which showed great dependence on the packing structure of DA monomers.[20] As shown in Figure 5(a), CD spectra for the (*Z*)-CNBE-PDA films polymerized with left- and right-handed CPUL clearly showed comparable but opposite responses for PDA chains as well as for CNBE units, with strong CD activity at 298, 413, 625, and 673 nm, assigned to the absorption of spiral CNBE cores and helical PDA backbone, respectively. Namely, the chiral information of CPUL could be transferred to CNBE central core via the spiral PDA backbone. The helical morphologies of self-assembled (Z)-CNBE-DA after irradiation with CPUL were demonstrated by the TEM images (Supporting Information Fig. S11). However, upon irradiation with nonpolarized UV light, no CD signal for PDA chains or for CNBE units could be detected [Fig. 5(a)iii)]. The (*Z*)-CNBE-DA had a planar molecular configuration, conducive to ordered closely molecular packing arrangement. The topochemical polymerization of the diacetylene units occurred via 1,4-addition reaction, as a result of specific rotations of the monomeric units relative to the positions of their centers of mass. In the π-conjugated PDA backbone, the π-orbital overlap is altered by rotation of the C—C bonds in the backbone, causing the change of the planar configuration of PDA backbone.[41] In the case of normal UV irradiation, the rotation direction of C—C bonds within PDA backbone were random; thus, the film exhibited no macroscopical CD signals. Upon irradiation with CPUL, the rotation direction of C—C bonds within PDA backbone would follow the rotational direction of CPUL due to the special interaction between CPUL and the diacetylene dimer. Therefore, one kind of helical PDA backbone were predominantly formed and the film exhibited obvious CD signals. Based on above results, a possible mechanism for the formation of helical assemblies in the crystal state upon CPUL irradiation could be proposed to explain this phenomenon [Fig. 5(b)].

Meanwhile, the (*Z*)-CNBE-PDA films exhibited completely reversible thermochromic phase transition behavior with a recoverable blue-to-red color change when the heating treatment temperature was below 80 °C [Fig. 6(a)].[42] Interestingly, optically chirality was maintained during the thermochromics phase transition. As illustrated in Figure 6(b), CD signal for PDA chains exhibited corresponding blue-shift, similar as those in the UV absorption band, while CD signal for CNBE units remained almost unchanged. When

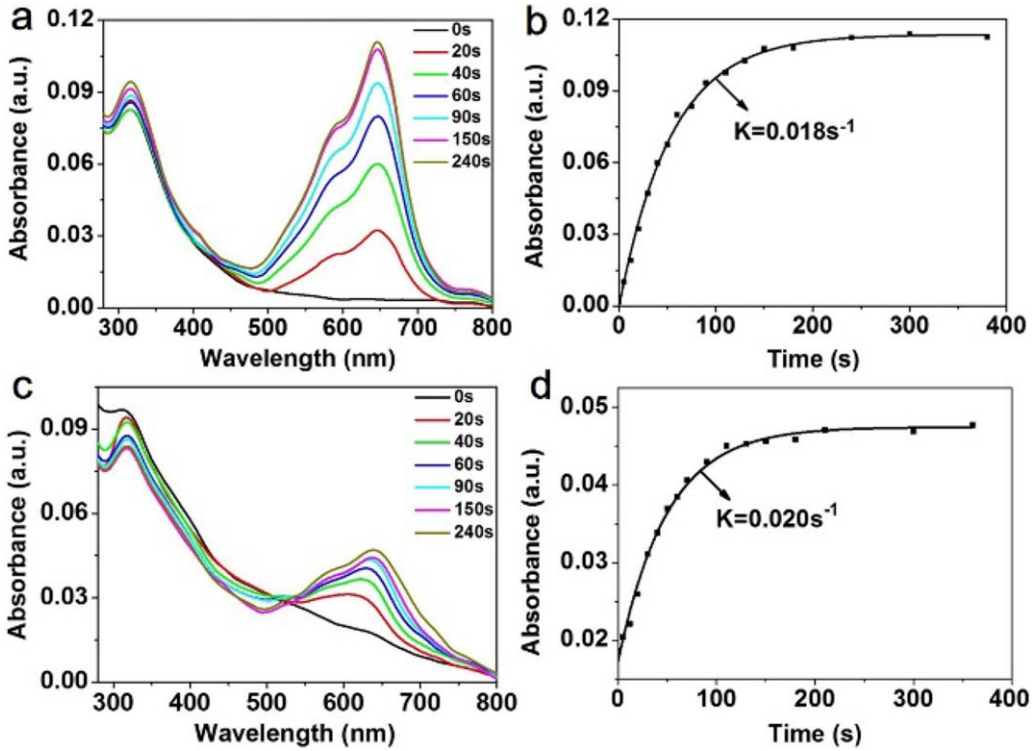

FIGURE 4 Time-resolved development of (a) UV–vis absorption spectra and (b) absorption maximum at 645 nm for the (*Z*)-CNBE-DA films upon 254-nm UV irradiation. Time-resolved development of (c) UV–vis absorption spectra and (d) absorbance at 645 nm for the (*E*)-CNBE-DA films upon 254-nm UV irradiation. The irradiation intensity was about 0.07 mW·cm^{-2}. [Color figure can be viewed at wileyonlinelibrary.com]

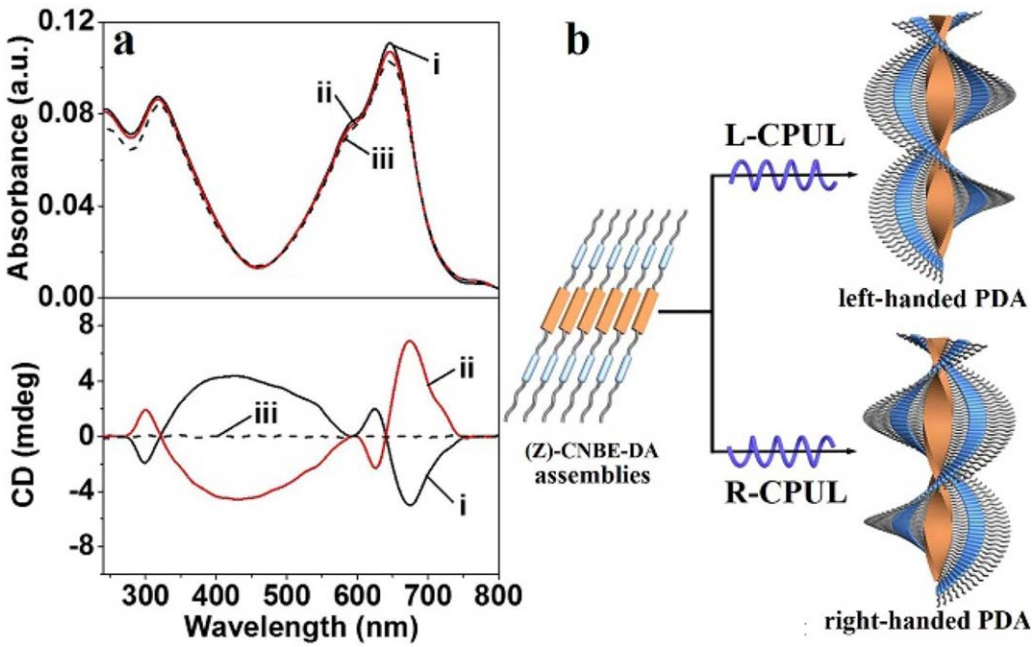

FIGURE 5 (a) UV–vis absorption spectra and CD spectra of (*Z*)-CNBE-DA films after irradiation with (i) left-handed CPUL, (ii) right-handed CPUL, and (iii) nonpolarized UV light. (b) The formation mechanism of the helical (*Z*)-CNBE-PDA assemblies in the crystal state upon CPUL irradiation. The irradiation intensity was about 14 mW·cm^{-2}. [Color figure can be viewed at wileyonlinelibrary.com]

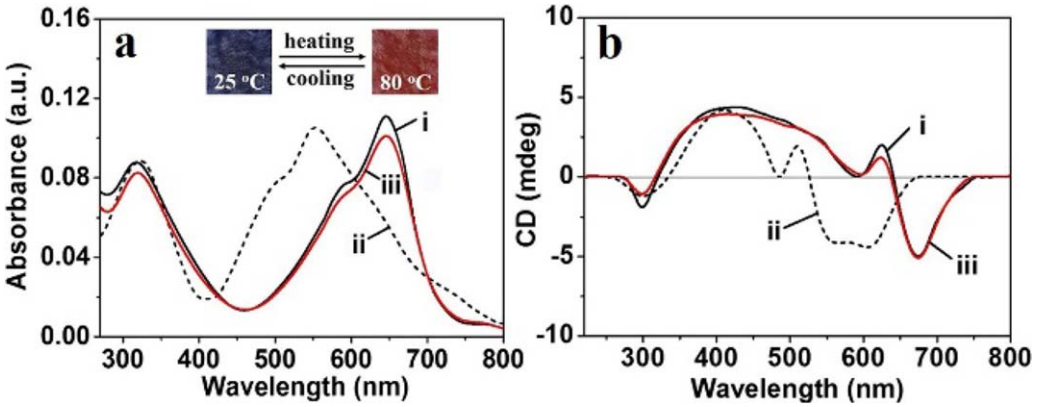

FIGURE 6 (a) UV–vis absorption spectra and (b) CD spectra of (*Z*)-CNBE-PDA films at 25 °C (i), heating to 80 °C (ii), and then cooling to 25 °C (iii). The inset in (a) showed the reversible color change for (*Z*)-CNBE-PDA films upon heating treatment. [Color figure can be viewed at wileyonlinelibrary.com]

cooling to room temperature, CD signal for PDA chains could return to the original position. All above results indicated that this enantioselective polymerization of (*Z*)-CNBE-DA films should be a deterministic process, and the handedness of applied CPUL directed the helical direction of PDA chain and the helical packing arrangement of CNBE cores.

As for the sample pretreated with 365-nm UV light irradiation, partial (*Z*)-CNBE-DA molecules were turned into the *E*-isomer. Although the sample could be polymerized upon CPUL irradiation, no obvious CD signal for PDA chains or for CNBE units could be detected, indicating that the ordered helical PDA chains or helical packing arrangement of CNBE cores could not be formed in this case (Supporting Information Fig. S12). The disordered loose molecular packing arrangement could be obtained due to the complicated intermolecular steric hindrance within the bent-shaped *E*-isomers. Therefore, the sample exhibited CD silence in this case.

Furthermore, it should be noted here that no obvious change in the structure, morphology, and chirality for the CNBE-DA sample after polymerization could be observed when treated with 365-nm or 254-nm light. The polymerization ensured "locking" of the chain configuration, and inhibited the photoisomerization of the CNBE units in this case. Namely, the molecular stacking arrangement and the resulting optical properties (e.g., absorption, chirality) could firstly be easily controlled through the *Z*/*E* isomerization by the external light stimuli, and then be permanently locked through polymerization of adjacent DA moieties by light. Therefore, the entire process of the control of molecular stacking arrangement and the locking of resulting optical properties could be solely manipulated by light.

CONCLUSIONS

In summary, a novel photo-responsive α-cyanostilbene-functionalized diacetylene monomer was synthesized, and the effect of *Z*/*E* isomerization for the CNBE core on the mesomorphic, polymerization, and chirality induction behavior were explored in detail. The rod-like (*Z*)-CNBE-DA assemblies exhibited nematic LC phase with a wide temperature range between 178 and 91 °C, while no LC phase could be observed for the bent-shaped (*E*)-CNBE-DA assemblies. (*Z*)-CNBE-DA had a planar molecular configuration, favoring the topo-polymerization and formation of helical PDA chains upon CPUL irradiation. However, the intermolecular steric hindrance and irregular loose packing within (*E*)-CNBE-DA assemblies inhibited the topo-polymerization and formation of helical PDA chains. This work not only provides an extended effort toward molecular stacking engineering but also is of great fundamental value for the rational design of novel PDA assemblies toward practically smart photonic devices and sensors.

ACKNOWLEDGMENTS

This research was carried out with funds from the National Natural Science Foundation of China (21574120), and Science and Technological Fund of Anhui Province for Outstanding Youth (1608085J01).

REFERENCES AND NOTES

1 J. Kim, J. Lee, W. Y. Kim, H. Kim, S. Lee, H. C. Lee, Y. S. Lee, M. Seo, S. Y. Kim, *Nat. Commun.* **2015**, *6*, 6959.

2 L. Zhu, X. Li, Q. Zhang, X. Ma, M. Li, H. Zhang, Z. Luo, H. Agren, Y. Zhao, *J. Am. Chem. Soc.* **2013**, *135*, 5175–5182.

3 M. Deng, L. Zhang, Y. Jiang, M. Liu, *Angew. Chem. Int. Ed.* **2016**, *55*, 15062–15066.

4 Z. Shen, T. Wang, M. Liu, *Angew. Chem. Int. Ed.* **2014**, *53*, 13424–13428.

5 S. J. Yoon, J. H. Kim, K. S. Kim, J. W. Chung, B. Heinrich, F. Mathevet, P. Kim, B. Donnio, A. J. Attias, D. Kim, S. Y. Park, *Adv. Funct. Mater.* **2012**, *22*, 61–69.

6 B. K. An, G. Johannes, S. Y. Park, *Acc. Chem. Res.* **2012**, *45*, 544–554.

7 D. Y. Kim, S. A. Lee, M. Park, K. U. Jeong, *Chemistry* **2015**, *21*, 545–548.

8 W. Hu, Y. Chen, H. Jiang, J. Li, G. Zou, Q. Zhang, D. Zhang, P. Wang, H. Ming, *Adv. Mater.* **2014**, *26*, 3136–3141.

9 M. Ulaganathan, R. V. Hansen, N. Drayton, H. Hingorani, R. G. Kutty, H. Joshi, S. Sreejith, Z. Liu, J. Yang, Y. Zhao, *ACS Appl. Mater. Interfaces* **2016**, *8*, 32643–32648.

10 G. Yang, Y. Zhang, H. Xia, G. Zou, Q. Zhang, *RSC Adv.* **2016**, *6*, 53794–53799.

11 G. Yang, W. Hu, H. Xia, G. Zou, Q. Zhang, *J. Mater. Chem. A* **2014**, *2*, 15560.

12 X. Chen, G. Zhou, X. Peng, J. Yoon, *Chem. Soc. Rev.* **2012**, *41*, 4610–4630.

13 Y. Zhu, D. Qiu, G. Yang, M. Wang, Q. Zhang, P. Wang, H. Ming, D. Zhang, Y. Yu, G. Zou, R. Badugu, J. R. Lakowicz, *Biosens. Bioelectron.* **2016**, *85*, 198–204.

14 D. E. Wang, Y. Zhang, T. Li, Q. Tu, J. Wang, *RSC Adv.* **2014**, *4*, 16820.

15 D. H. Park, W. Jeong, M. Seo, B. J. Park, J. M. Kim, *Adv. Funct. Mater.* **2016**, *26*, 498–506.

16 S. R. Diegelmann, J. D. Tovar, *Macromol. Rapid Commun.* **2013**, *34*, 1343–1350.

17 Y. Li, K. M. Wong, H. L. Wong, V. W. Yam, *ACS Appl. Mater. Interfaces* **2016**, *8*, 17445–17453.

18 D. Y. Kim, S. A. Lee, D. Jung, K. U. Jeong, *Sci. Rep.* **2016**, *6*, 28659.

19 S. R. Diegelmann, N. Hartman, N. Markovic, J. D. Tovar, *J. Am. Chem. Soc.* **2012**, *134*, 2028–2031.

20 Y. Xu, H. Jiang, Q. Zhang, F. Wang, G. Zou, *Chem. Commun.* **2014**, *50*, 365–367.

21 J. W. Park, S. Nagano, S.-J. Yoon, T. Dohi, J. Seo, T. Seki, S. Y. Park, *Adv. Mater.* **2014**, *26*, 1354–1359.

22 J. W. Chung, B.-K. An, S. Y. Park, *Chem. Mater.* **2008**, *20*, 6750–6755.

23 L. Zhu, Y. Zhao, *J. Mater. Chem. C* **2013**, *1*, 1059–1065.

24 X. Wang, Z. Gao, J. Zhu, Z. Gao, F. Wang, *Polym. Chem.* **2016**, *7*, 5217–5220.

25 B.-K. An, S.-K. Kwon, S.-D. Jung, S. Y. Park, *J. Am. Chem. Soc.* **2002**, *124*, 14410–14415.

26 Z. Zhao, J. W. Y. Lam, B. Z. Tang, *Soft Matter* **2013**, *9*, 4564.

27 J. Seo, J. W. Chung, J. E. Kwon, S. Y. Park, *Chem. Sci.* **2014**, *5*, 4845–4850.

28 J. W. Chung, S.-J. Yoon, B.-K. An, S. Y. Park, *J. Phys. Chem. C* **2013**, *117*, 11285–11291.

29 M. Martinez-Abadia, B. Robles-Hernandez, M. R. de la Fuente, R. Gimenez, M. B. Ros, *Adv. Mater.* **2016**, *28*, 6586–6591.

30 P. Xing, H. Chen, M. Ma, X. Xu, A. Hao, Y. Zhao, *Nanoscale* **2016**, *8*, 1892–1896.

31 M. Yang, P. Xing, M. Ma, Y. Zhang, Y. Wang, A. Hao, *Soft Matter* **2016**, *12*, 6038–6042.

32 Y. Jin, Y. Xia, S. Wang, L. Yan, Y. Zhou, J. Fan, B. Song, *Soft Matter* **2015**, *11*, 798–805.

33 L. Zhu, C. Y. Ang, X. Li, K. T. Nguyen, S. Y. Tan, H. Agren, Y. Zhao, *Adv. Mater.* **2012**, *24*, 4020–4024.

34 X. Tong, Y. Zhao, B. K. An, S. Y. Park, *Adv. Funct. Mater.* **2006**, *16*, 1799–1804.

35 M. Martínez-Abadía, B. Robles-Hernández, B. Villacampa, M. R. de la Fuente, R. Giménez, M. B. Ros, *J. Mater. Chem. C* **2015**, *3*, 3038–3048.

36 H. J. Kim, D. R. Whang, J. Gierschner, S. Y. Park, *Angew. Chem. Int. Ed.* **2016**, *55*, 15915–15919.

37 H. Nam, B. Boury, S. Y. Park, *Chem. Mater.* **2006**, *18*, 5716–5721.

38 B. Veeraprakash, N. P. Lobo, T. Narasimhaswamy, A. B. Mandal, *Phys. Chem. Chem. Phys.* **2015**, *17*, 19936–19947.

39 Y. Ren, W. H. Kan, M. A. Henderson, P. G. Bomben, C. P. Berlinguette, V. Thangadurai, T. Baumgartner, *J. Am. Chem. Soc.* **2011**, *133*, 17014–17026.

40 K. U. Jeong, S. Jin, J. J. Ge, B. S. Knapp, M. J. Graham, J. J. Ruan, M. M. Guo, H. M. Xiong, F. W. Harris, S. Z. D. Cheng, *Chem. Mater.* **2005**, *17*, 2852–2865.

41 R. W. Carpick, D. Y. Sasaki, M. S. Marcus, M. A. Eriksson, A. R. Burns, *J. Phys.: Condens. Matter* **2004**, *16*, R679–R697.

42 S. Lee, J. Lee, M. Lee, Y. K. Cho, J. Baek, J. Kim, S. Park, M. H. Kim, R. Chang, J. Yoon, *Adv. Funct. Mater.* **2014**, *24*, 3699–3705.